International Journal of Mechanical, Industrial and Aerospace Sciences
ISSN: 2517-9950
Vol:8, No:8, 2014

Natural Convection in Wavy-Wall Cavities Filled with Power-Law Fluid

Cha'o-Kuang Chen, Ching-Chang Cho

***Abstract*—**This paper investigates the natural convection heat transfer performance in a complex-wavy-wall cavity filled with power-law fluid. In performing the simulations, the continuity, Cauchy momentum and energy equations are solved subject to the Boussinesq approximation using a finite volume method. The simulations focus specifically on the effects of the flow behavior index in the power-law model and the Rayleigh number on the flow streamlines, isothermal contours and mean Nusselt number within the cavity. The results show that pseudoplastic fluids have a better heat transfer performance than Newtonian or dilatant fluids. Moreover, it is shown that for Rayleigh numbers greater than $Ra=10^3$, the mean Nusselt number has a significantly increase as the flow behavior index is decreased.

***Keywords*—**Non-Newtonian fluid, Power-law fluid, Natural convection, Heat transfer enhancement, Cavity, Wavy wall.

I. Introduction

NATURAL convection in regular cavities (e.g., square or rectangular) is of importance in many engineering systems, such as electronic cooling devices, heat exchangers, MEMS devices, electric machinery, solar energy collectors, and so on [1]. Natural convection in irregular cavities, e.g., wavy-wall cavities, is also important for many applications due to the potential for an enhanced heat transfer performance.

Mahmud et al. [2] examined the natural convection phenomenon within a cavity bounded by two isothermal wavy walls and two adiabatic straight walls. Oztop et al. [3] investigated the problem of natural convection within wavy-wall cavities with a volumetric heat source. Cho et al. [4] investigated the natural convection heat transfer performance within a cavity with complex-wavy-wall surfaces. Overall, the results presented in [2]-[4] show that the flow characteristics and heat transfer performance in wavy-wall cavities depend strongly on both the geometry parameters of the wavy surface and the flow parameters.

The studies described above all consider a Newtonian fluid. However, in many engineering applications (e.g., oil drilling, slurry transport, paper making, food processing, polymer engineering, and so on), the fluid is non-Newtonian. As a result, the natural convection heat transfer performance of non-Newtonian fluids has also attracted significant attention in the literature. For example, Kim et al. [5] investigated the transient buoyant convection of a power-law fluid within a square cavity. The results showed that the rheological property of the power-law fluid had a significant effect on the flow behavior and heat transfer performance within the cavity under both transient and steady-state conditions; particularly under high Rayleigh numbers and low Prandtl numbers. Lamsaadi et al. [6] studied the natural convection heat transfer performance of power-law fluids enclosed within a shallow horizontal rectangular cavity uniformly heated from one side. The results showed that given a high Prandtl number and a cavity with a large aspect ratio, the heat transfer behavior was dominated by the flow behavior index of the power-law fluid and the Rayleigh number. Lamsaadi et al. [7] investigated the natural convection heat transfer characteristics of power-law fluids enclosed in a tilted shallow rectangular cavity. The results further showed that for a large aspect ratio and a high Prandtl number, the heat transfer performance depended on the inclination angle of the cavity. Turan et al. [8] investigated the natural convection behavior of power-law fluids in a square cavity with differentially-heated side walls. It was shown that the mean Nusselt number increased with an increasing Rayleigh number, but decreased with an increasing flow behavior index. Khezzar et al. [9] studied the natural convection heat transfer performance of power-law fluids in a rectangular inclined cavity. The results showed that shear-thinning and shear-thickening fluids improved and reduced the heat transfer performance, respectively, compared to that obtained using a Newtonian fluid.

The studies in [5]-[9] all consider the natural convection heat transfer of non-Newtonian fluids within regular cavities. However, as mentioned earlier, the heat transfer characteristics of non-Newtonian fluids enclosed within wavy-wall cavities are also an important concern in many practical engineering problems. Accordingly, the present study performs a numerical investigation into the natural convection heat transfer performance of non-Newtonian fluids within a cavity comprising left and right walls with complex-wavy surfaces and a constant high and low temperature, respectively, and upper and lower horizontal walls with an insulated condition. The simulations focus specifically on the effects of the flow behavior index and the Rayleigh number on the flow streamlines, isothermal contours and mean Nusselt number within the cavity.

II. Mathematical Formulation

Fig. 1 illustrates the complex-wavy-wall cavity considered in the present study. As shown, the cavity has a width and a height. The related mathematical formulations and numerical solution procedure are described in the following.

C. K. Chen is with the Department of Mechanical Engineering, National Cheng Kung University, Tainan 701, Taiwan, ROC (phone: +886-6-2757575-62140; fax: +886-6-2342081; e-mail: ckchen@mail.ncku.edu.tw).

C. C. Cho is with the Department of Vehicle Engineering, National Formosa University, Yunlin 632, Taiwan, ROC (e-mail:cccho@nfu.edu.tw).

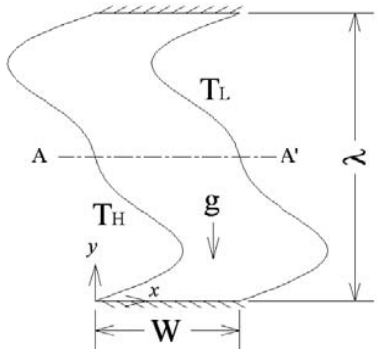

Fig. 1 Schematic illustration of complex-wavy-wall cavity

A. Governing Equations

The flow behavior and heat transfer characteristics in the cavity shown in Fig. 1 are governed by the continuity equation, the Cauchy momentum equation and the energy equation. To simplify the governing equations, the following assumptions are made: (i) the fluid within the cavity is incompressible and laminar; (ii) the thermophysical properties of the fluid are all constant other than the density which varies in accordance with the Boussinesq approximation; (iii) the flow and temperature fields are two-dimensional and steady state; and (iv) the thermal radiation and viscous dissipation effects are sufficiently small to be ignored. Given these assumptions, the governing equations can be written as follow:

$$\nabla \cdot \vec{V} = 0 \tag{1}$$

$$\rho(\vec{V}\cdot\nabla)\vec{V} = -\nabla P + \nabla\cdot\mu[\nabla\vec{V} + (\nabla\vec{V})^{\text{þ}} + \rho g\beta(T - T_L)\vec{j} \tag{2}$$

$$(\vec{V}\cdot\nabla T) = \alpha\nabla^2 T \tag{3}$$

where the superscript denotes transposition. Note that the last term in (2) represents the buoyancy body force and acts in the y-direction.

In performing the simulations, the rheological behavior of the non-Newtonian fluid within the cavity is described using a power-law model. In other words, the apparent viscosity term in (2) is expressed as [10]

$$\mu = m\dot{\gamma}^{n-1} \tag{4}$$

where m is the flow consistency index, n is the flow behavior index and $\dot{\gamma}$ is the shear rate. Given a flow behavior index of $n > 1$, the fluid is said to be dilatant. Conversely, given a flow behavior index of $n < 1$, the fluid is said to be pseudoplastic. Finally, for a flow behavior index of $n = 1$, the fluid is said to be Newtonian.

When investigating the problem of natural convection within a cavity filled with non-Newtonian fluid, two non-dimensional parameters must be defined, namely the generalized Rayleigh number (Ra) and the generalized Prandtl number ($\Pr$), i.e., [5], [9].

$$Ra = \frac{g\beta(T_H - T_L)W^3}{\alpha(\frac{m}{\rho})^{\frac{1}{2-n}} W^{\frac{2(1-n)}{2-n}}} \tag{5}$$

$$\Pr = \frac{(\frac{m}{\rho})^{\frac{1}{2-n}} W^{\frac{2(1-n)}{2-n}}}{\alpha} \tag{6}$$

The convection heat transfer performance can be quantified via the Nusselt number (Nu), i.e.

$$Nu = \frac{hW}{k} \tag{7}$$

where k is the thermal conductivity and $h$is the convection heat transfer coefficient. The mean Nusselt number along the hot wavy-wall surface can then be obtained as

$$Nu_m = \frac{1}{l_w}\int_0^{\lambda} Nud\eta \tag{8}$$

where l_w is the length of the hot wavy-wall.

B. Boundary Conditions

In defining the boundary conditions for the governing equations described above, it is assumed that the left wavy-wall has a constant high temperature (T_H), while the right wavy-wall has a constant low temperature (T_L). In addition, the top and bottom walls are assumed to be flat and perfectly insulated. Finally, a no-slip impermeable velocity boundary condition is applied at all of the wall surfaces.

C. Wavy-Wall Geometry and Numerical Solution Procedure

In performing the simulations, the profile of the wavy-wall surface was modeled as follows

$$\frac{x}{W} = 0.5Sin(\frac{2\pi y}{\lambda}) + 0.2Sin(\frac{4\pi y}{\lambda}) \tag{9}$$

where λ is the wavelength. Moreover, the body-fitted grid system used to model the wavy-wall surface was generated by solving a set of Poisson equations [11].

The governing equations given in (1)-(3) are expressed in terms of a Cartesian coordinate system. However, the wavy-wall surface given in (9) is expressed in terms of a non-orthogonal system. Hence, (1)-(3) cannot be solved directly. Thus, in performing the simulations, the governing equations were transformed to the following generalized form [10]

$$\begin{aligned}&\frac{\partial}{\partial\xi}(\rho_\varphi Uf) + \frac{\partial}{\partial\eta}(\rho_\varphi Vf) = \frac{\partial}{\partial\xi}[\frac{\Gamma_\varphi}{J}(\alpha_\varphi\frac{\partial f}{\partial\xi} - \beta_\varphi\frac{\partial f}{\partial\eta})]\\ &+\frac{\partial}{\partial\eta}[\frac{\Gamma_\varphi}{J}(-\beta_\varphi\frac{\partial f}{\partial\xi} + \gamma_\varphi\frac{\partial f}{\partial\eta})] + JS_\varphi\end{aligned} \tag{10}$$

where f is a generalized variable; ξ and η are the two axes of the transformed coordinate system; U and V are the velocity components in the transformed coordinate system; S_ϕ is a source term; α_ϕ, β_ϕ and γ_ϕ are the parameters of the transformed coordinate system; and J is the Jacobian factor.

The governing equations and corresponding boundary conditions were discretized using the finite-volume numerical method [12]. The convection terms in the governing equations were discretized using the second-order upwind scheme. The velocity-pressure fields were coupled using the SIMPLE C algorithm [12]. The discretized algebraic equations were solved iteratively using a line-by-line TDMA scheme.

D.Numerical Validation

To validate the numerical model and solution procedure described above, the results obtained for the mean Nusselt number in a square cavity filled with pseudoplastic fluids with various values of the flow behavior index were compared with those presented in [5], [8] given different values of the Prandtl number. Note that the left and right walls of the cavity were assumed to be maintained at different temperatures, while the top and bottom walls were both assumed to be insulated. The results presented in Fig. 2 show that the calculated results for are in close agreement with those presented in [5], [8] for all values of the Prandtl number and flow behavior index. In other words, the validity of the numerical model is confirmed.

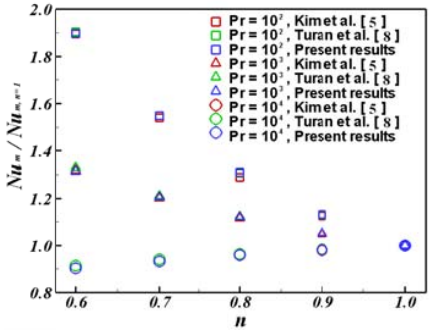

Fig. 2 Comparison of present results with published results for variation of mean Nusselt number with flow behavior index given various values of Prandtl number. Note that $Nu_{m,n=1}$ indicates the mean Nusselt number of a Newtonian fluid. Note also that the results relate to a simple square cavity with $Ra = 10^6$

III. Results and Discussion

In performing the simulations, the parameters were specified as follows: Rayleigh number, from $Ra = 10^1$ to $Ra = 10^6$; Prandtl number, $\Pr = 6.8$; and wavelength of wavy surface, $\lambda = 2W$.

Fig. 3 shows the flow streamlines within the complex-wavy wall cavity for various flow behavior indexes and Rayleigh numbers. Figs. 4 (a) and (b) illustrate the corresponding non-dimensional *u*-velocity profiles at cross-section $A-A'$ (i.e., the midpoint position of the wavy surface, see Fig. 1). It is seen in Figs. 3 (a)~(c) that at low Rayleigh numbers (i.e., $Ra = 10^3$), an elliptical recirculation structure is formed in the center of the cavity for all considered values of the flow behavior index due to the buoyancy effect induced by the difference in the temperatures of the left and right cavity walls, respectively. Under low Rayleigh number conditions, a low flow velocity and perturbation effect is induced, and thus heat transfer occurs primarily as the result of conduction. However, at higher values of the Rayleigh number ($Ra = 10^6$), the flow velocity induced by the buoyancy effect is increased. As a result, the flow streamlines within the cavity become twisted, and thus the heat transfer mechanism transits from one of conduction to one of convection. In addition, comparing the results presented in Figs. 3 (d)-(f) with those presented in Figs. 3 (a)-(c), it is seen that the flow streamlines are more densely packed in the region of the wavy-wall surface. In other words, the velocity gradient within the cavity is increased under higher Rayleigh number conditions. Therefore, a higher shear rate is induced.

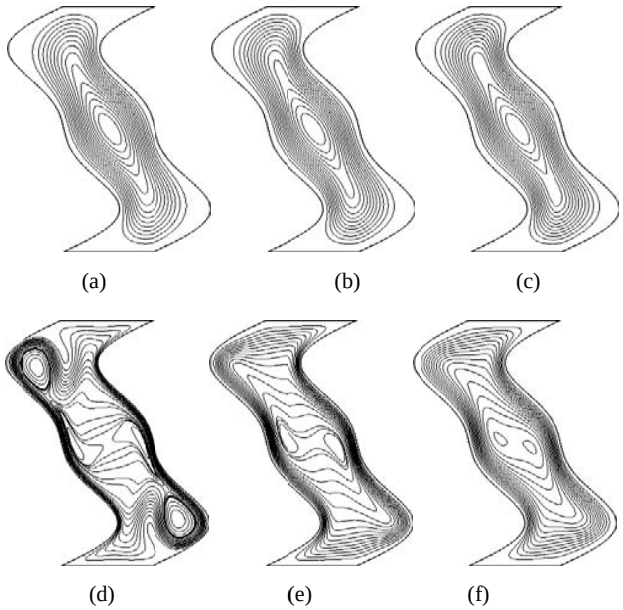

Fig. 3 Flow streamlines given Rayleigh number of $Ra = 10^3$ and flow behavior indexes of: (a) $n = 0.7$, (b) $n = 1.0$ and (c) $n = 1.3$; and flow streamlines given Rayleigh number of $Ra = 10^6$ and flow behavior indexes of: (d) $n = 0.7$, (e) $n = 1.0$ and (f) $n = 1.3$

For a small value of the Rayleigh number, the flow recirculation structure has only a weak intensity, and thus the apparent viscosity is approximately equal for all three fluids. As a result, the flow streamlines for the pseudoplastic fluid (Fig. 3 (a)) and dilatant fluid (Fig. 3 (c)) are similar to those for the Newtonian fluid (Fig. 3 (b)). However, as shown in Fig. 4 (a), the pseudoplastic fluid has a slightly higher velocity component than the dilatant or Newtonian fluid due to its inherent shear-thinning property. For a higher Rayleigh number, the shear rate within the cavity is increased, and thus a notable difference in the flow structures of the three fluids is observed.

For the pseudoplastic fluid, the enhanced shear rate leads to a significant decrease in the apparent viscosity and a significant increase in the fluid velocity, and thus the thermal-induced buoyancy effect results in a complex flow structure characterized by the formation of two high-intensity recirculation structures (Fig. 3 (d)). However, for the dilatant fluid, the higher shear rate prompts an increasing of the apparent viscosity, and thus a less pronounced twisting of the flow streamlines occurs. Consequently, the non-dimensional *u*-velocity profile of the dilatant fluid at cross-section $A-A'$ is less that of the Newtonian fluid (see Fig. 4 (b)).

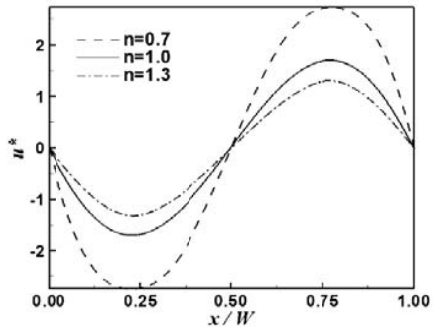

(a)

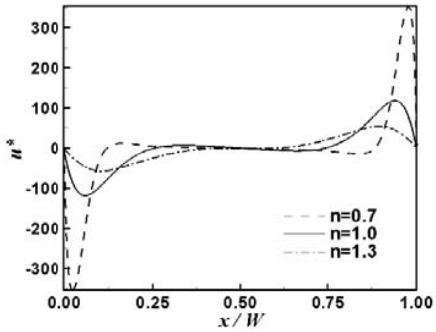

(b)

Fig. 4 Distribution of u-velocity along *x*-direction at $y/W=1.0$ (i.e., cross-section $A-A'$ in Fig. 1) given (a) Rayleigh number of $Ra=10^3$ and (b) Rayleigh number of $Ra=10^6$. Note that $u^*(=uW/\alpha)$ is the non-dimensional velocity component

Fig. 5 shows the isothermal contours within the complex-wavy wall cavity for various flow behavior indexes and Rayleigh numbers. Fig. 6 plots the corresponding results for the non-dimensional temperature profile at cross-section $A-A'$ of the wavy-wall cavity. As described above, given a low value of the Rayleigh number, the conduction mechanism dominates the heat transfer process within the cavity for all considered values of the flow behavior index. As a result, the isothermal contours essentially follow the profile of the wavy surface (see Figs. 5 (a)-(c)) and the temperature profile within the cavity has a linear-like distribution (see Fig. 6). Given a larger value of the Rayleigh number, a greater buoyancy effect is induced, and thus the flow perturbation effect is enhanced. As a result, the isothermal contours within the cavity become twisted (see Figs. 5 (a)-(f)) and the temperature profile has a non-linear distribution (see Fig. 6). For the pseudoplastic fluid ($n=0.7$), the viscosity reduces significantly under higher Rayleigh number conditions due to its inherent shear-thinning property and gives rise to a stronger flow perturbation effect. Consequently, the thickness of the thermal boundary layer reduces and an improved heat transfer performance is obtained. Conversely, the viscosity of the dilatant fluid increases, and thus the perturbation effect is reduced. As a consequence, the thickness of the thermal boundary layer increases and the heat transfer performance is correspondingly reduced.

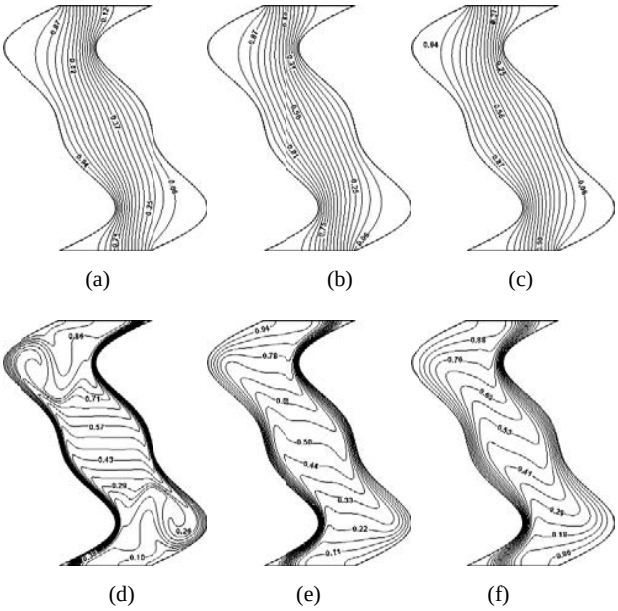

(a) (b) (c)

(d) (e) (f)

Fig. 5 Isothermal contours given Rayleigh number of $Ra=10^3$ and flow behavior indexes of: (a) $n=0.7$, (b) $n=1.0$ and (c) $n=1.3$; and isothermal contours given Rayleigh number of $Ra=10^6$ and flow behavior indexes of: (d) $n=0.7$, (e) $n=1.0$ and (f) $n=1.3$. Note that the isotherm data shown in the figures are non-dimensional values

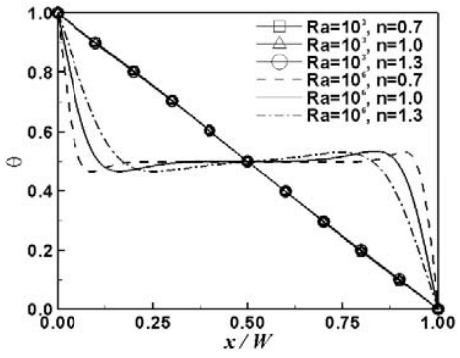

Fig. 6 Distribution of non-dimensional temperature along x-direction at $y/W=1.0$ (i.e., cross-section $A-A'$ in Fig. 1). Note that the dimensionless temperature is defined as $\theta=\dfrac{T-T_L}{T_H-T_L}$

Fig. 7 shows the variation of the mean Nusselt number with the Rayleigh number as a function of the flow behavior index (n). It is seen that for all values of n , the mean Nusselt number has a low and constant value for Rayleigh numbers lessthan $Ra = 10^3$. This result is to be expected since under low Rayleigh number conditions, the buoyancy effect induces only performance is dominated by the conduction mechanism; irrespective of the fluid viscosity. However, as the Rayleigh number increases, the flow perturbation effect also increases. Consequently, the conduction mechanism transits to a convection mechanism, and thus the heat transfer performance is correspondingly improved. As described earlier in relation to Figs. 3-6, the viscosity of the pseudoplastic fluid is lower than that of the dilatant fluid. Hence, the pseudoplastic fluid experiences a greater flow perturbation effect than the dilatant fluid. Consequently, in the convection-dominated regime, the mean Nusselt number increases with a decreasing flow behavior index.

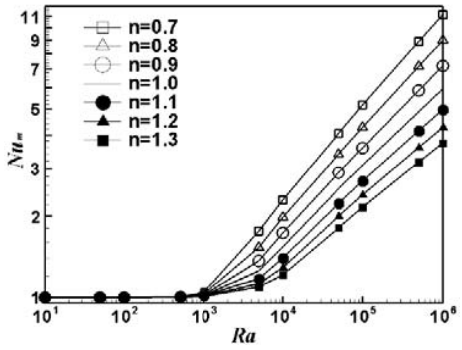

Fig. 7 Variation of mean Nusselt number with Rayleigh number as function of flow behavior index

IV. Conclusions

This study has investigated the natural convection heat transfer performance within a complex-wavy-wall cavity filled with non-Newtonian fluid. In modeling the cavity, it has been assumed that the vertical walls have a complex wavy surface and different temperatures, while the horizontal walls are flat and insulated. Furthermore, in performing the simulations, the natural convection characteristics within the cavity have been described by means of the continuity equation, Cauchy momentum equation, energy equation and Boussinesq approximation, while the rheological behavior of the non-Newtonian fluid has been characterized using a power-law model. The simulations have focused specifically on the effects of the flow behavior index and Rayleigh number on the flow streamlines, isothermal contours and mean Nusselt number within the cavity. The results have shown that for Rayleigh numbers greater than $Ra = 10^3$, the mean Nusselt number has a significantly increase as the flow behavior index is decreased. Moreover, the mean Nusselt number is insensitive to the Rayleigh number in the conduction-dominated regime, but increases with an increasing Rayleigh number in the convection-dominated regime.

Acknowledgment

The authors would like to thank the National Science Council of the Republic of China, Taiwan, for financially supporting this research under Contract No. 101-2221-E-006-092-MY2. In addition, the authors wish to thank Prof. Robert J. Poole for supplying the source data used in Fig. 3, respectively, for reference purposes.

References

[1] S. Ostrach, “Natural convection in enclosures,” J. Heat Transf.-Trans. ASME, vol. 110, pp. 1175-1190, 1988.
[2] S. Mahmud, P.K. Das, N. Hyder, and A.K.M.S., Islam, “Free convection in an enclosure with vertical wavy walls,” Int. J. Therm. Sci., vol. 41, pp. 440-446, 2002.
[3] H.F. Oztop, E. Abu-Nada, Y. Varol, and A. Chmkha, “Natural convection in wavy enclosures with volumetric heat sources,” Int. J. Therm. Sci., vol. 50, pp. 502-514, 2011.
[4] C.C. Cho, C.L. Chen, and C.K. Chen, “Natural convection heat transfer performance in complex-wavy-wall enclosed cavity filled with nanofluid,” Int. J. Therm. Sci., vol. 60, pp. 255-263, 2012.
[5] G.B. Kim, J.M. Hyun, and H.S. Kwak, “Transient buoyant convection of a power-law non-Newtonian fluid in an enclosure,” Int. J. Heat Mass Transf., vol. 46, pp. 3605-3617, 2003.
[6] M. Lamsaadi, M. Naimi, and M. Hasnaoui, “Natural convection heat transfer in shallow horizontal rectangular enclosures uniformly heated from the side and filled with non-Newtonian power law fluids,” Energy Conv. Manag., vol. 47, pp. 2535-2551, 2006.
[7] M. Lamsaadi, M. Naimi, M. Hasnaoui, and M. Mamou, ”Natural convection in a titled rectangular slot containing non-Newtonian power-law fluids and subject to a longitudinal thermal gradient,” Numer. Heat Tranf. A-Appl., vol. 50, pp. 561-583, 2006.
[8] O. Turan, A. Sachdeva, N. Chakraborty, and R.J. Poole, “Laminar natural convection of power-law fluids in a square enclosure with differentially heated side walls subjected to constant temperatures,” J. Non-Newton. Fluid Mech., vol. 166, pp. 1049-1063, 2011.
[9] L. Khezzar, D. Siginer, and I. Vinogradov, “Natural convection of power law fluids in inclined cavities,” Int. J. Therm. Sci., vol. 53, pp. 8-17, 2012.
[10] C.C. Cho, C.L. Chen, and C.K. Chen, “Electrokinetically-driven non-Newtonian fluid flow in rough microchannel with complex-wavy surface,” J. Non-Newton. Fluid Mech., vol. 173-174, pp. 13-20, 2012.
[11] P.D. Thomas, and J.F. Middlecoff, “Direct control of the grid point distribution in meshes generated by elliptic equations,” AIAA J., vol. 18, pp. 652-656, 1980.
[12] S. V. Patankar, “Numerical Heat Transfer and Fluid Flow,” New York:McGraw-Hill, 1980.

Prof. Cha’o-Kuang Chen is currently National Chair Professor of Mechanical Engineering Department at National Cheng Kung University, Tainan, Taiwan, ROC. He received his B.S. degree in mechanical engineering from National Cheng Kung University, Tainan, Taiwan, in 1958, his Master of Mechanical Engineering from Georgia Institute of Technology, Atlanta, Ga., in 1970, and his Ph.D. in mechanical engineering from the University of Liverpool, UK, in 1986. He was the head of the Department of Mechanical Engineering in 1990–1993. His current research interests include nonlinear stability analysis of Newtonian and non-Newtonian fluid flows, thermal stability analysis of electro-magneto-fluids, finite-time thermodynamic cycles and thermal efficiency analysis, fuzzy control and optimal design, molecular dynamics simulation, nanotechnology, heat/mass transfer in micro/nano-scales, thermal economics, and Lattice Boltzmann method. He has published over 500 SCI papers in international journals

Dr. Ching-Chang Cho is currently an assistant professor of Vehicle Engineering Department at National Formosa University, Yunlin, Taiwan, ROC. He received his Ph.D. in mechanical engineering from National Cheng Kung University, Taiwan, in 2009. His major research areas include electroosmotic flow, micromixer, non-Newtonian fluid and heat/mass transfer enhancement. He has published over 20 SCI papers in international journals.